Sensors and Actuators A 194 (2013) 259–268

Contents lists available at SciVerse ScienceDirect

Sensors and Actuators A: Physical

journal homepage: www.elsevier.com/locate/sna

A detailed study on current–voltage characteristics of Au/n-GaAs in wide temperature range

E. Özavcı, S. Demirezen*, U. Aydemir, Ş. Altındal

Physics Department, Faculty of Sciences, Gazi University, 06500 Ankara, Turkey

ARTICLE INFO

Article history:
Received 16 September 2012
Received in revised form 6 February 2013
Accepted 12 February 2013
Available online 19 February 2013

Keywords:
Au/GaAs Schottky diodes
I–V characteristics
Barrier height
Inhomogeneous barrier

ABSTRACT

In order to obtain the detailed information on the conduction mechanisms of the Au/n-GaAs Schottky barrier diode (SBD), the current–voltage (*I–V*) characteristics were carried out in the temperature range of 80–340 K by the steps of 20 K. The ideality factor (n) decreases, while the effective barrier height (Φ_{Bo}) increases with increasing temperature (80–340 K). The semilogarithmic *I–V* curve is almost parallel for each temperature. Therefore, its slope and tunneling parameter (E_{oo}) remained almost constant as independent of temperature with an average of 27.47 V^{-1} and 28.04 meV, respectively. Furthermore, the reverse saturation current (I_s) ranges, indication that the charge transport mechanism in the Au/n-GaAs SBD is tunneling due to the weak temperature dependence of the I_s. Thus, it can be said that the experimental *I–V* data quite well obey the thermionic field emission (TFE) model especially at low temperatures rather than the other transport mechanisms. On the other hand, an abnormal decrease in the Φ_{Bo} and increase in the n with decreasing temperature have been observed which leads to non-linearity in the activation energy plots and a linear relationship between the barrier heights (BHs) and the ideality factors of the SBD. The high value of n especially at low temperatures cannot be also explained only TFE theory. Therefore, we tried to explain the non-ideal behavior of the forward-bias *I–V* characteristics in Au/n-GaAs SBD with the basis of a thermionic emission (TE) mechanism with a Gaussian distribution (GD) of the BHs. The obtained results show that the temperature dependence of forward bias *I–V* characteristics of the Au/n-GaAs SBD can be successfully explained in terms of the TE mechanism with a double GD of BHs for low bias region (LBR) and moderate bias region (MBR).

1. Introduction

Gallium arsenide (GaAs) is one of the advantageous semiconductors for high-speed and low-power devices. However, the performance of GaAs based devices, including metal–semiconductor (MS) or metal–insulator–semiconductor (MIS) type Schottky barrier diodes (SBDs), field effect transistors (FETs) and heterostructure bipolar transistors (HBTs), especially depends on the surface and interface defect density (Nss), series resistance (R_s), temperature and applied bias voltage [1–18]. It is well known, standard TE theory predicts that the Φ_b independent from temperature. However, temperature dependence of the extracted BH and nonlinearity of Richardson plot have been observed for over six decades [2] in the form of the T_o anomaly [4,7]. More recently, inhomogeneity of the BH has been proposed [19,20] as an explanation for nonlinearity and it has been applied to a wide variety of diodes [4–18,21–24]. In addition, in detail survey of the literature reveals that there are conflicting measurements concerning especially the temperature dependence of both the n and the Φ_b in GaAs based and other SBDs [1–18]. Among them, Padovani and Sumner [2] reported that in Au n-type GaAs SBDs the value of n decreased with increasing temperature and Padovani [3], concluded in later publication that Φ_b should decrease linearly with increasing temperature. Hackam and Harrop [7] proposed that the n should also be included in the expression for the reverse saturation current (I_s). Thus, this a modification, which results in good agreement between the values of the Φ_b obtained from both *I–V* and *C–V* methods over a wide temperature range. Hudait et al. [4] and Bengi et al. [5] show that the analysis of the forward bias *I–V* characteristics in GaAs-based SBDs based on TE theory mechanism has revealed an abnormal increase of Φ_b and decrease of n, especially at low temperatures. Such behavior of Φ_b and n with temperature was interpreted on the basis of the existence of Gaussian distribution of the SBHs around a mean value due to SBH inhomogeneities prevailing at the M/S interface. On the other hand, Ozdemir et al. [9] and Altuntas et al. [11], show that double Gaussian.

In most cases, the experimental *I–V* characteristics of real Schottky diodes significantly deviate from ideal ones calculated

* Corresponding author. Tel.: +90 312 2021276; fax: +90 312 2122279.
E-mail addresses: s.demirezen@gazi.edu.tr, selcukdemirezen@gmail.com (S. Demirezen).

0924-4247/$ – see front matter © 2013 Elsevier B.V. All rights reserved.
http://dx.doi.org/10.1016/j.sna.2013.02.018

from commonly used the TE and diffusion theories [25,26]. The current-transport mechanism in these devices such as MS, MIS and solar cells are dependent on various parameters such as the process of surface preparation, BH inhomogeneity at M/S interface, impurity concentration of a semiconductor, density of interface states or defects, R_s of device, device temperature and applied bias voltage. It is well known the change in main electrical parameters becomes also important especially at low temperatures. While thermionic field emission (TFE) and field emission (FE) mechanisms became dominant in these temperatures, thermionic emission (TE) became dominant above room temperature. Therefore, the investigation of conduction mechanism especially in high doped and with large and moderate forbidden band gap semiconductor such as SiC, GaN and GaAs and very low temperatures is very important.

However, a simultaneous contribution from two or more mechanisms could also be possible [27]. Nevertheless, the analyses of the *I–V* characteristics of these devices at room temperature alone does not give detailed information about their current transport mechanisms and the nature of formation BH at M/S interface [19–27]. The temperature dependence of the forward bias *I–V* characteristics allows the identification of the different current transport mechanism and formation of BH at M/S interface. Therefore, in the present study, the *I–V* characteristics of Au/n-GaAs SBDs were measured in the temperature range of 80–340 K by steps of 20 K. Nonlinearity of the Richardson plot, high value of *n* and positive temperature coefficient in BH have been explained on the basis of the existence of a Gaussian distribution of the BHs around a mean value due to BH inhomogeneities at the M/S interface.

2. Experimental method

Au/n-GaAs SBDs were fabricated n-GaAs of the 5.08 cm diameter and (1 0 0) orientation n-GaAs wafer having thickness of about 350 μm with $\sim 2 \times 10^{18}$ cm^{-3} dopant concentrations. For the fabrication process, the firstly n-GaAs wafer was dipped in ammonium peroxide for 40 s to remove native oxide layer on the surface. Then, the GaAs wafer was etched in sequence with acid solutions (H_2SO_4:H_2O_2:H_2O = 3:1:1) for 60 s, and (HCl:H_2O = 1:1) for another 60 s. After, the substrate is again rinsed in deionized water with 18 MΩ. Finally, it was dried by nitrogen. After surface of n-GaAs cleaning high purity Au (99.995%) with a thickness of ~1500 Å was thermally evaporated from the tungsten filament on to the whole back side of the n-GaAs wafer at a pressure of $\sim 10^{-6}$ Torr in vacuum pump system. In order to perform the low resistivity ohmic contact, Au coated wafer was sintered at 400 °C for 5 min in a nitrogen atmosphere. After that, circular dots of 1 mm in diameter and 1500 Å thick high purity Au rectifying contacts were deposited on the surface of the n-GaAs wafer through a metal shadow mask in high vacuum system in the pressure of about 10^{-6} Torr. The metal thickness and deposition rates were monitored with the help of quartz crystal thickness monitor. The wafer was mounted on a copper holder with the help of silver dag and the electrical contacts were made to the upper electrodes by the use of tiny silver coated wires with silver paste. The schematic diagram of the Au/n-GaAs SBD was given in Fig. 1. The forward and reverse bias *I–V* measurements were performed by the use of a Keithley 2400 source meter in the temperature range of 80–340 K by the steps of 20 K using a temperature-controlled Janis vpf-475 cryostat, which enabled us to make measurements in the temperature range of 77–450 K. The sample temperature was always monitored by using a Lake Shore model 321 auto-tuning temperature controllers with sensitivity better than ±0.1 K. All measurements were carried out with the help of a microcomputer through an IEEE-488 AC/DC converter card.

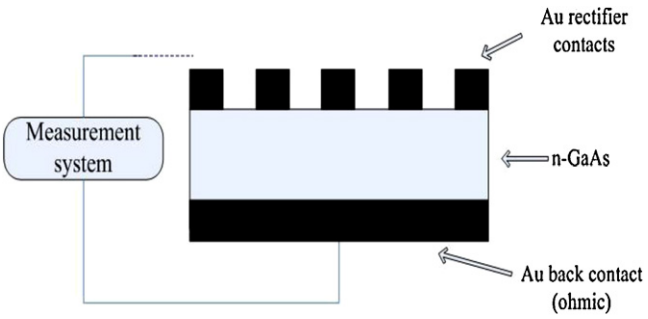

Fig. 1. Schematic diagram of the Au/n-GaAs SBD and measurement system.

3. Results and discussion

3.1. Analysis of current–voltage (I–V) characteristics in the low bias region (LBR)

Fig. 2. shows the semi-logarithmic forward bias *I–V* characteristics of Au/n-GaAs SBD in the temperature range of 80–340 K by steps of 20 K. As can be seen from Fig. 2, the *I–V* plot for each temperature has two distinct linear regions with different slopes which are corresponding to low bias region ($V \leq 0.3$ V) and moderate bias region ($\sim 0.35\ V < V \leq 0.8$ V). In addition, in the high bias region (HBR) ($V > 0.8$ V), there is a deviation from the linearity in the forward bias *I–V* plot due to the effect of series resistance (R_s).

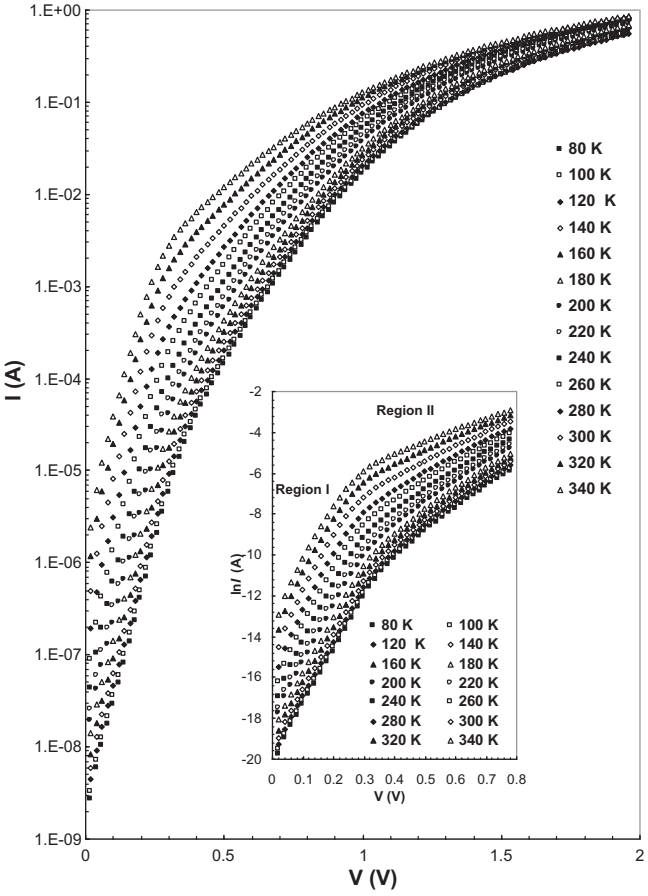

Fig. 2. The semi-logarithmic forward bias *I–V* characteristics of the Au/n-GaAs SBD at various temperatures.

Table 1
Temperature dependent values of I_s, n, Φ_{Bo} and $n\Phi_{Bo}$ for Au/nGaAs SBD obtained from the forward bias I–V characteristics.

T (K)	Region I (low bias region)				Region II (moderate bias region)			
	I_o (A)	n	Φ_{Bo} (eV)	$n\Phi_{Bo}$ (eV)	I_o (A)	n	Φ_{Bo} (eV)	$n\Phi_{Bo}$ (eV)
80	1.16×10^{-9}	5.43	0.18	1.00	3.82×10^{-7}	12.33	0.14	1.77
110	2.31×10^{-9}	3.91	0.25	0.98	4.73×10^{-7}	9.07	0.20	1.83
120	3.01×10^{-9}	3.58	0.27	0.98	6.30×10^{-7}	8.44	0.22	1.84
140	4.10×10^{-9}	3.05	0.32	0.98	8.86×10^{-7}	7.38	0.25	1.88
160	5.72×10^{-9}	2.65	0.36	0.97	1.28×10^{-6}	6.59	0.29	1.91
180	9.27×10^{-9}	2.37	0.41	0.96	1.96×10^{-6}	6.02	0.32	1.94
200	1.35×10^{-8}	2.09	0.45	0.94	3.10×10^{-6}	5.58	0.35	1.98
220	1.89×10^{-8}	1.87	0.49	0.91	4.72×10^{-6}	5.23	0.39	2.01
240	3.31×10^{-8}	1.70	0.53	0.89	8.51×10^{-6}	5.02	0.41	2.07
260	7.19×10^{-8}	1.57	0.56	0.87	1.84×10^{-5}	4.96	0.43	2.14
280	1.63×10^{-7}	1.47	0.58	0.86	4.13×10^{-5}	5.00	0.45	2.25
300	4.41×10^{-7}	1.40	0.60	0.84	1.11×10^{-4}	5.22	0.46	2.40
320	1.11×10^{-6}	1.34	0.62	0.83	2.91×10^{-4}	5.54	0.47	2.59
340	2.32×10^{-6}	1.29	0.64	0.83	6.38×10^{-4}	5.84	0.48	2.79

These two regions in Fig. 2 were called LBR and MBR, respectively. When the diode has a series resistance (R_s) and n is greater than unity, the relationship between current and voltage ($V \geq 3kT/q$), according to the TE mechanism, is given by [25,26]

$$I = \underbrace{AA^*T^2 \exp(-q\Phi_{Bo}/kT)}_{I_s}\left[\exp\left(\frac{q(V-IR_s)}{nkT}\right)-1\right] \quad (1)$$

where, the pre-factor is the reverse saturation current (I_s) and the other A, A^*, Φ_{Bo}, V, T, k, n, IR_s quantities are the diode area, effective Richardson constant and equals to 8.16 A/cm^2 K^2 for n-type GaAs [5], effective BH, applied bias voltage, absolute temperature in K, Boltzmann's constant, ideality factor and the voltage across on R_s, respectively. For the LBR and MBR, the n and I_s values are determined from the slope and intercept of the linear regions of ln I versus V plot using Eq. (1) for each temperature. The Φ_{Bo} was calculated using theoretical value A^* (8.16 A/cm^2 K^2) and extrapolated I_s for each temperature according to

$$\Phi_{Bo} = \frac{kT}{q}\ln\left(\frac{AA^*T^2}{I_s}\right) \quad (2)$$

The temperature dependent I_s, n, Φ_{Bo} and $n\Phi_{Bo}$ values determined from the I–V plots of Au/n-GaAs SBD were given in Table 1 for each bias region. As can be seen in Table 1 and Fig. 3(a) and (b), n and Φ_{Bo} values of Au/n-GaAs SBD are strong function of temperature and they ranged from 5.43 and 0.18 eV (at 80 K) and 1.29 and 0.64 eV (at 340 K), respectively. The value of n decreases with increasing temperature and such behavior is in agreement with literature. On the other hand, the value of Φ_{Bo} shows an unusual behavior that it increases with increasing temperature. It is well known, such temperature dependence of BH for two regions is an obvious disagreement with the reported negative temperature coefficient of the BH and forbidden band gap of semiconductor.

As can be seen in, Fig. 2 the ln I–V plots in the temperature range of 80–340 K are almost parallel in the LBR rather than MBR and, consequently, the diode ideality factor for LBR is not constant with temperature. On the other hand the nT is almost constant. Similar results have been reported by various researchers [5,28–30]. As can be seen in Table 1 and Fig. 4, for the LBR, the change in n with temperature was found to change linearly with inverse temperature as

$$n(T) = n_0 + \frac{T_0}{T} \quad (3)$$

where n_o and T_o are constants which were found to be 0.07 and 436.3 K, respectively. These results show that the value of n should also be included in the expression for the I_s. The high value of n for two regions can be attributed to the existence of an interfacial

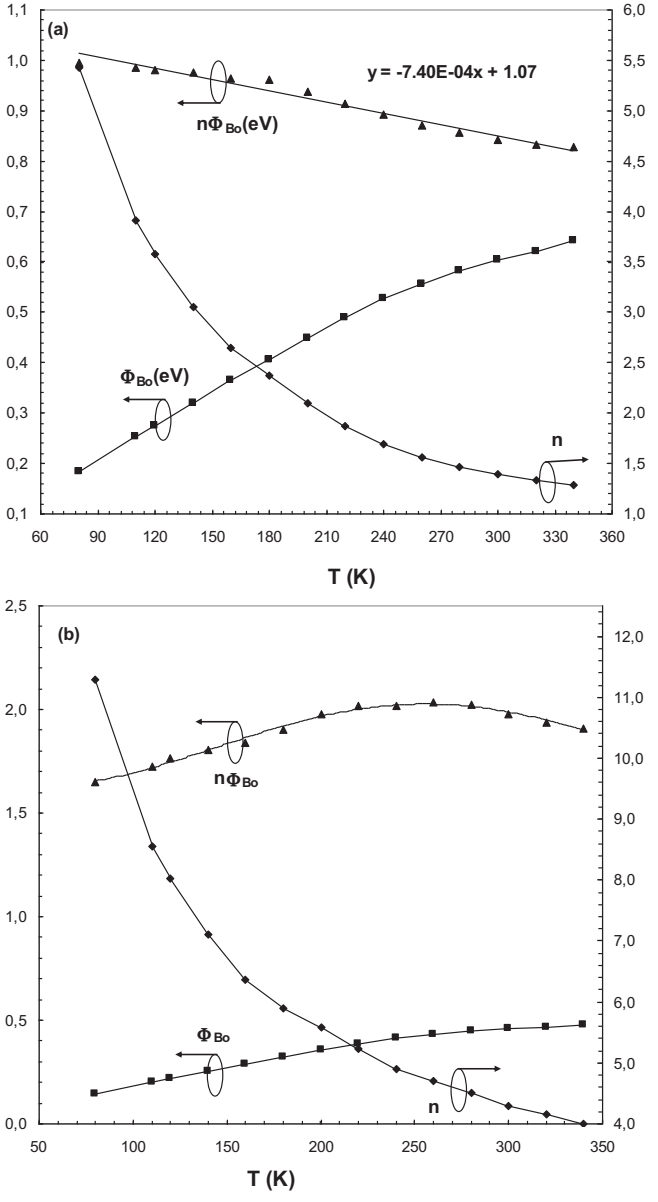

Fig. 3. The temperature dependence of n, Φ_{Bo} and $n\Phi_{Bo}$ of Au/n-GaAs SBD obtained from the forward bias I–V data for (a) LBR and (b) MBR for various temperatures.

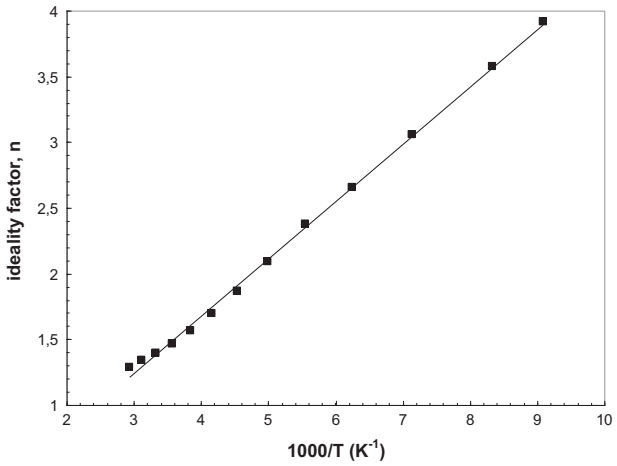

Fig. 4. The plot of n versus $1000/T$ of the Au/n-GaAs SBD for LBR.

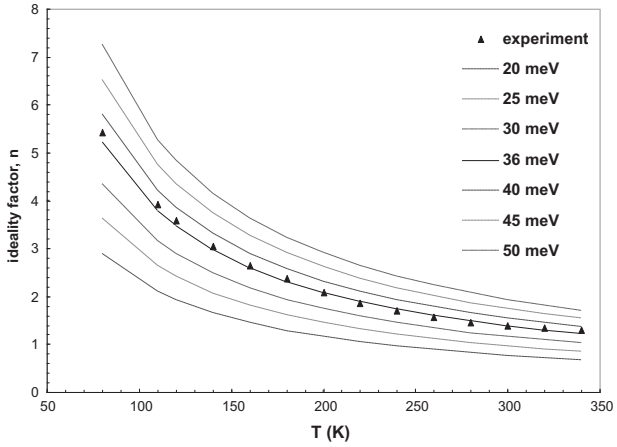

Fig. 5. The variation of ideality factor with temperature for the Au/n-GaAs SBD.

layer native or deposited, image force lowering, the charges at traps/interface states and barrier inhomogeneity [5–13,16–20]. Thus, the modified value of BH can be expressed as [7]

$$\Phi_B = n(T)\frac{kT}{q}\ln\left(\frac{AA^*T^2}{I_s}\right) = n(T)\Phi_{Bo} \tag{4}$$

After this modification, as can be seen in Table 1 and Fig. 4, the value of Φ_B decreases almost linearly with the temperature as

$$\Phi_B = \Phi_B(0K) + \alpha T \tag{5}$$

Here the barrier height at absolute temperature Φ_B (0 K) and the temperature coefficient of the barrier height α are experimentally found to be 1.07 eV and 7.4×10^{-4} eVK^{-1} respectively. It is clear that the negative temperature coefficient of BH is in good agreement with the negative coefficient of GaAs (5.4×10^{-4} eVK^{-1}) [26]. On the contrary to LBR, in MBR region the $n\Phi_{Bo}$ values increase with increasing temperature especially at low and moderate temperatures and it becomes decrease at high temperatures. Such double region of $\ln I$ versus V plots can also be explained by two diode models in the literature [31–35]. However for two bias regions, the increase in BH with T cannot explain with TE theory and it will be explained in following sections as double Gaussian BH.

It is well known, the predominant current transport or conduction mechanisms are also dependent on various other parameters such as process of surface preparation, formation of oxide layer native or deposited and BHs at M/S interface. As can be seen from Table 1 and Fig. 3(a) and (b), the decrease in Φ_{Bo} and increase in the n with decreasing temperatures point to a deviation from the pure TE theory, suggesting that the tunneling current mechanisms such as thermionic field emission (TFE) or field emission (FE) possibly warrant consideration. If the current transport is controlled by the TFE or FE theory, the relationship between the forward bias voltage and current can be expressed as [2,3,25–28]

$$I = I_{tun}\left[\exp\left(\frac{q(V-IR_S)}{E_O}\right)-1\right], \tag{6a}$$

with

$$n_{tun} = \frac{E_{oo}}{kT}\coth\left(\frac{E_{oo}}{kT}\right) = \frac{E_o}{kT}, \tag{6b}$$

where E_{oo} is the characteristic tunneling energy that is related to the tunnel effect transmission probability:

$$E_{oo} = \frac{h}{4\pi}\left(\frac{N_D}{m_e^*\varepsilon_s}\right)^{1/2} \tag{6c}$$

where $h(=6.626\times10^{-34}$ J s) is Planck constant, $m_e{}^*(=0.067\,m_o)$ is effective mass of electron, $\varepsilon_s(=13.1\varepsilon_o)$ is the dielectric constant of GaAs, $\varepsilon_o(=8.85\times10^{-12}$ F/m) is the permittivity of vacuum. Thus, the value of E_{oo} was found as 28.04 meV. It is well known, TFE should be valid when $E_{oo}\approx kT/q$; the TE if $E_{oo}\ll kT/q$ and the FE if $E_{oo}\gg kT/q$. Thus, if the FE dominates, then the E_o will lie on straight line. In this case, E_o is independent of temperatures and E_o is equal to E_{oo}. Fig. 6(b) shows E_o ($=nkT/q$) versus kT/q plot of the Au/n-GaAs SBD in temperature range of 80–340 K. As shown from this figure, the value of E_o was obtained as 36 meV and this value is equal to E_{oo}. This $E_{oo}=36$ meV value corresponds to a doping concentration of 3.30×10^{18} cm^{-3}. The obtained experimental $E_{oo}(=36$ meV) value is close to possible theoretical value of 28.04 meV calculated form the initial electron concentration. When considering the bias coefficient of the barrier height, β, Eq. (6b) can be written as [2,3,36]

$$n_{tum} = \frac{E_o}{kT(1-\beta)} \tag{6d}$$

where $\beta = d\Phi_{Bo}/dV$. Fig. 5 represents the theoretical temperature dependence of the n when the current through BH is dominated by the TFE. The solid lines in Fig. 5 were obtained from Eq. 6(d) using different values of the characteristic energy, E_{oo}, without considering the bias coefficient of the barrier height, $\beta=0$. As can be seen from Fig. 5, the experimental temperature dependence of the n is in good agreement with the curve calculated for the Au/n-GaAs at $E_{oo}=36$ meV. Fig. 6a shows that, the $\ln I$ versus V plot have to linear region with different slope. On the other word, Fig. 6a reveals a linear relationship between the logarithm of reverse saturation current (I_s) and T. As can be seen in Fig. 2, the $\ln I$ versus V plot for low forward applied bias voltage are almost parallel in the whole temperature range, which can be well explained by TFE theory rather than the other theories.

On the other hand, in the MBR, there is an abnormal decrease in the Φ_{Bo} and an increase in the n with a decrease in temperature have been observed which leads to non-linearity in the activation energy plots and a linear relationship between the barrier heights and the ideality factors of the SBD. This increase in Φ_{Bo} with increasing temperature is against the negative temperature coefficient of band gap or BH in expected literature. The high value of ideality especially at low temperatures in our samples cannot be also explained the existence a native insulator layer and particular distribution of interface states at metal/semiconductor (M/S) interface. Therefore, we tried to explained the non-ideal behavior of the forward-bias I–V characteristics in the fabricated Au/n-GaAs SBD on the based on a TE mechanism theory with a double Gaussian distribution (GD) of the BHs.

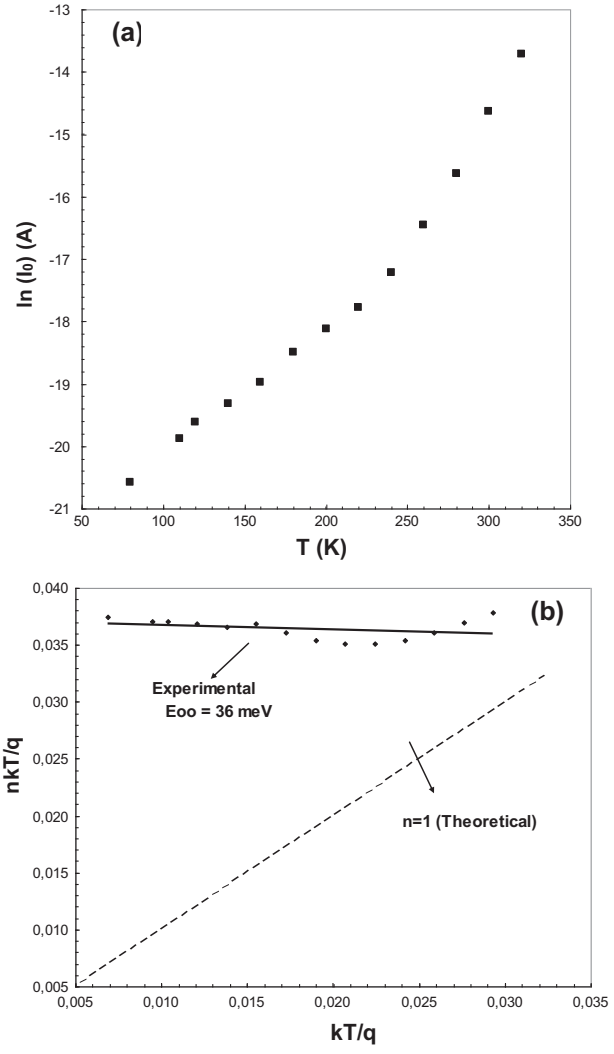

Fig. 6. Plots of the nkT/q versus kT/q of Au/n-GaAs SBD for LBR.

3.1.1. Inhomogeneous barrier analysis in the LBR

In order to explain the non-ideal behavior of the forward-bias I–V characteristics in the Au/n-GaAs SBD at LBR, we show the conventional activation energy/Richardson plot of $\ln(I_s/T^2)$ versus q/kT (Fig. 7). For the evaluation of the BH, one may also make use of the Richardson plot of saturation current. In Eq. (1), the I_s can be rearrange as

$$\ln\left(\frac{I_s}{T^2}\right) = \ln(AA^*) - \frac{q\Phi_{Bo}}{kT} \tag{7}$$

The conventional $\ln(I_s/T^2)$ versus q/kT plot in Fig. 7 shows two linear regions with different slopes. Such behavior of Richardson plot can be attributed to the spatially inhomogeneous BHs and potential fluctuations at the interface or two distinct conduction mechanisms [9,11,37–39]. As can be seen from Fig. 7, the $\ln(I_s/T^2)$ versus q/kT plot shows two distinct linear regions with different slopes and intercepts. In the first region (220–340 K), the values of the activation energy (E_a = BH) and A^* were obtained from the slope and intercept of this straight-line as 0.218 eV and 3.15×10^{-6} A/cm^2 K^2, respectively, while in the second region (80–200 K), the values of E_a and A^* were obtained as 0.006 eV and 5.1×10^{-11} A/cm^2 K^2, respectively. It is well known, for an electron, this value of A^* in Au/n-GaAs SBD is much lower than the theoretically value of 8.16 A/cm^2 K^2 for n-GaAs. Fig. 7 consists two BHs which are corresponding to the low and high barrier areas. That is, at low temperatures, the carrier

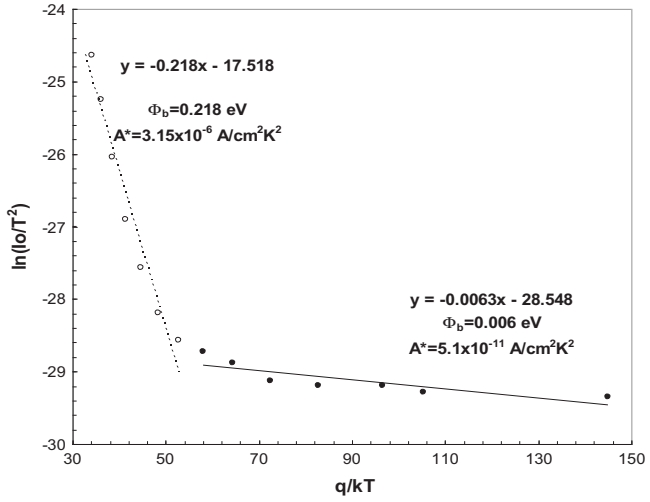

Fig. 7. Richardson plots of the $\ln(I_s/T^2)$ versus q/kT of Au/n-GaAs SBD for LBR.

transport across MS contact would be preferentially through the lower barriers in the potential distribution [11,37–39]. Horvath [39] explained that the A^* value obtained from the temperature dependence of the I–V characteristics may be affected by the lateral inhomogeneity of the barrier. Schmitsdorf et al. [40] used Tung's [19] theoretical approach and found a linear correlation between the experimental effective BHs and the ideality factors. Fig. 8 shows a plot of the experimental BH versus n and it shows also two linear regions with different slopes which can be explained by the lateral inhomogeneities of the BHs [11,40]. In the first region (220–340 K), the extrapolation of the experimental Φ_{Bo} and n plot for $n = 1$ has given the value of 0.708 eV. In the second region (80–200 K), the extrapolation of the Φ_{Bo} and n plot for $n = 1$ has given the value of 0.501 eV. Thus, it can be said that the decrease of the effective BH and increase of the n especially at low temperatures are possibly caused by the BH inhomogeneities.

In performing an analysis based on barrier inhomogeneity, we adopted the model of Werner and Güttler [20], introducing a GD in the BH with a mean value $\bar{\Phi}_{Bo}$ and standard deviation σ_s.

$$P(\Phi_B) = \frac{1}{\sigma_s\sqrt{2\pi}} \exp\left[-\frac{(\Phi_B - \bar{\Phi}_B)^2}{2\sigma_s^2}\right], \tag{8}$$

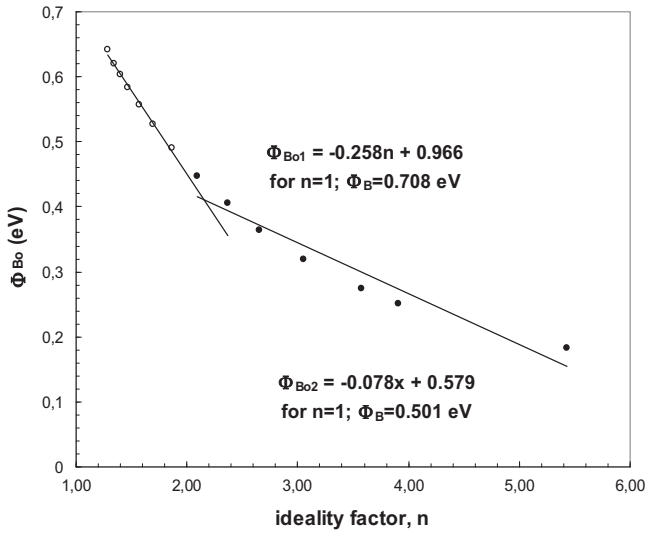

Fig. 8. Plot of the experimental BH versus n of Au/n-GaAs SBD for LBR.

where $1/(\sigma_s(2\pi)^{1/2})$ is the normalization constant of the Gaussian BH distribution. The total $I(V)$ across a SBD containing barrier inhomogeneities can be expressed as

$$I(V) = \int_{-\infty}^{+\infty} I(\Phi_B, V)P(\Phi_B)d\Phi, \quad (9)$$

where $I(\Phi_B,V)$ is the current at a bias (V) for a BH based on the ideal thermionic-emission-diffusion (TED) theory and $P(\Phi_B)$ is the normalized distribution function giving the probability of accuracy for BH. Performing this integration from $-\infty$ to $+\infty$, one can obtain the current $I(V)$ through an SB at a forward bias V as

$$I_o = AA^*T^2 \exp\left(\frac{-q\Phi_{ap}}{kT}\right) \quad (10)$$

$$I(V) = AA^*T^2 \exp\left[-\frac{q}{kT}\left(\bar{\Phi}_{Bo} - \frac{q\sigma_o^2}{2kT}\right)\right] \times \exp\left(\frac{qV}{n_{ap}kT}\right)\left[1 - \exp\left(-\frac{q(V - IRs)}{kT}\right)\right], \quad (11)$$

where Φ_{Bo} and n_{ap} are the apparent barrier height and apparent ideality factor, respectively and are given by [9,25]

$$\Phi_{ap} = \Phi_{Bo}(T = 0) - \frac{q\sigma_o^2}{2kT}, \quad (12)$$

$$\left(\frac{1}{n_{ap}} - 1\right) = \rho_2 - \frac{q\rho_3}{2kT}. \quad (13)$$

It is assumed that the modified SBH $\bar{\Phi}_{Bo}$ and σ_s are linearly bias dependent on Gaussian parameters, such as $\bar{\Phi}_B = \bar{\Phi}_{Bo} + \rho_2 V$ and standard deviation $\sigma_s = \sigma_{so} + \rho_3 V$, where ρ_2 and ρ_3 are voltage coefficients which may depend on temperature and they quantify the voltage deformation of the BH distribution [9,20]. The temperature dependence of σ_s is usually small and can be neglected [37–40].

In order to obtain an evidence of a GD of BHs, the experimental Φ_{ap} versus $q/2kT$ and n_{ap} versus $q/2kT$ plots (Fig. 9) was drawn by means of the data obtained from Fig. 2 respond to two lines instead of a single straight line with transition occurring at 200 K. Fitting the experimental I–V data gives Φ_{ap} and n_{ap}, respectively, which should obey Eqs. (11) and (12). Thus, the plot of Φ_{ap} versus $q/2kT$ (Fig. 9) gives a straight line and its intercept at the ordinate and slope giving Φ_{Bo} and zero-bias standard deviation (σ_s), respectively. The above observations indicate that the presence of double GD of BHs in the contact area. When the dots have been considered, the intercept and slope of this straight lines given two sets of values of Φ_{Bo} and σ_s as 0.92 eV and 0.127 V in the temperature range of 220–340 K (the distribution 1), and as 0.59 eV and 0.077 V in the temperature range of 80–200 K (the distribution 2). As can be seen from the Φ_{ap} versus $q/2kT$, σ_s value for the slope of the distribution 1 is larger than the distribution 2. Therefore it can be said that the distribution of BH for region 1 is wider from the region 2. In recently, such behavior of the double GD also was reported in the literature [9,11,42–43]. These changes were ascribed to the chemical treatment of the semiconductor surface during the cleaning of surface of semiconductor [41,42]. Likewise, as also indicated by Chand and Kumar [43], the existence of a double GD in the M/S contacts can be attributed to the nature of the inhomogeneities themselves in the two cases. This may involve variation in the interface composition, interface quality, electrical charges and non-stoichiometry, etc. Similarly, as can be clearly seen from Fig. 9b, the plot of $(n_{ap}^{-1} - 1)$ versus $q/2kT$ should also possess different characteristics in the two temperature ranges because of the diode contains two BH distributions. The values of ρ_2 obtained from the intercepts of the experimental $(n_{ap}^{-1} - 1)$ versus $q/2kT$ plot are −0.22 V in 220–340 K range (the distribution 1) and −0.38 V in 80–200 K range (the distribution 2), whereas the values of ρ_3 from the slopes are 0.0259 V in 220–340 K range and 0.0065 V in 80–200 K range. The linear behavior of this plot demonstrates that the n indeed expresses the voltage deformation of the GD of the SBH [19,20]. As can be seen from the $(n_{ap}^{-1} - 1)$ versus $q/2kT$, ρ_3 value or the slope of the distribution 1 is larger than the distribution 2. Therefore, we may point out that the distribution 1 is wider and relatively higher BH with bias coefficients ρ_2 and ρ_3 being smaller and larger, respectively. Thus, we can say that the distribution 2 at very low temperatures may possibly arise due to some phase change taking place on cooling below a certain temperature.

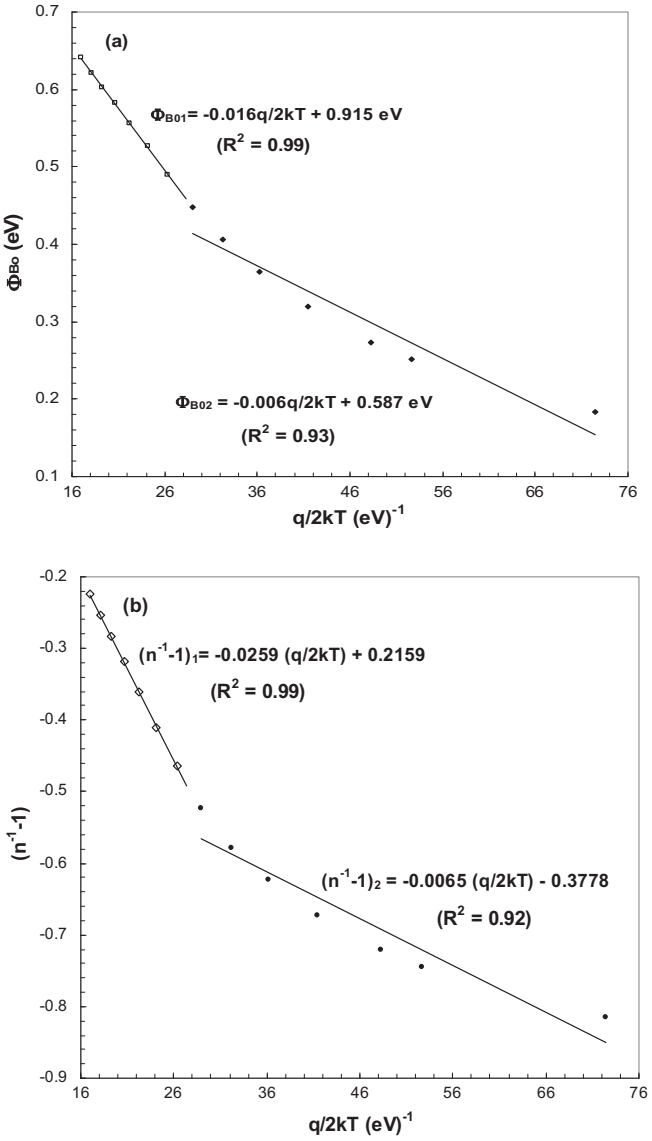

Fig. 9. (a) The apparent BH (Φ_{Bo} (I–V)) versus $q/2kT$ plot and (b) the ideality factor $(n^{-1} - 1)$ versus $q/2kT$ plot of Au/n-GaAs SBD for LBR.

As can be seen from Figs. 3(a) (Φ_{Bo} vs T), (b) (n vs T), 7 ($\ln I_s/T^2$ vs q/kT), 8 (Φ_{Bo} vs n) and 9 ($n^{-1} - 1$) versus $q/2kT$), there are two distinct straight lines with different slopes. These results show that the BH is depend on temperature and two different current transport mechanisms or two different mean BHs may dominate in measured temperature range. As a result, the predominant current transport is not only the TE and FE in our samples; rather, there are also two Gaussian distributions (GD1) and (GD2) BHs in the constant area

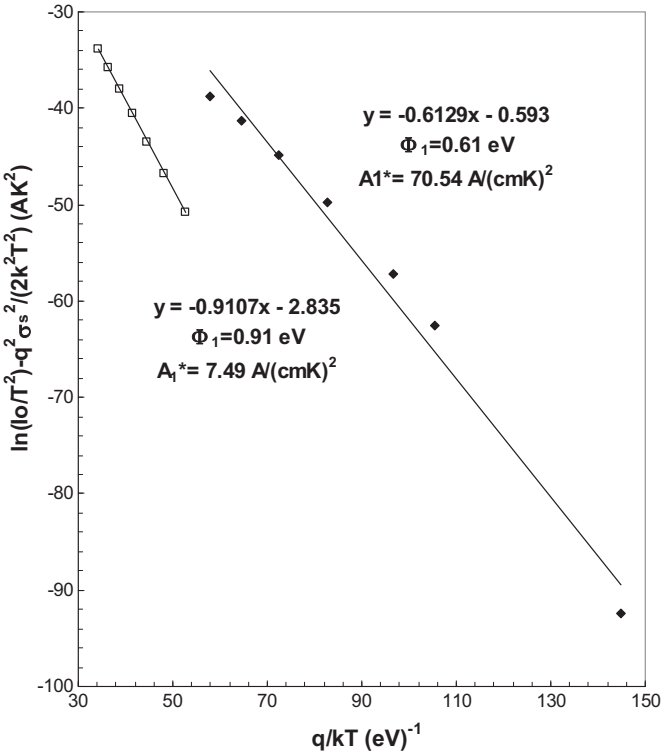

Fig. 10. Modified Richardson $\ln(I_s/T^2) - q^2\sigma_0^2/2k^2T^2$ versus. q/kT plot of Au/n-GaAs SBD for LBR according to GD of BHs.

which corresponding the high and low temperatures, respectively. Furthermore, the temperature range covered by each straight line suggests the regime where the corresponding distribution is effective [43]. All of these results implies that the investigation of the electrically influence of the *I–V* characteristics of the Schottky diodes is very important especially at low temperatures. Thus, *I–V* measurements at very low temperatures are capable of revealing the nature of barrier inhomogeneities present in the contact area.

As indicated above, the conventional activation energy $ln(I_s/T^2)$ versus q/kT plot has showed two linear regions. T_o explain these discrepancies, according to the Gaussian distribution of the BH, we can rewritten as

$$\ln\left(\frac{I_s}{T^2}\right) - \left(\frac{q^2\sigma_o^2}{2k^2T^2}\right) = \ln(AA^*) - \frac{q\Phi_{Bo}}{kT} \quad (14)$$

and a modified activation energy plot from this expression is obtained. Using the experimental I_s data, a modified $\ln(I_s/T^2) - q^2\sigma^2/2k^2T^2$ versus q/kT plot (Fig. 10) can be obtained according to Eq. (14) and should give a straight line with slope directly yielding the mean Φ_{Bo} and the intercept ($= \ln AA^*$) at the ordinate determining A^* for a given diode area A. The $\ln(I_s/T^2) - q^2\sigma^2/2k^2T^2$ values were calculated for both two values of σ_s obtained for the temperature ranges of 80–200 K and 220–340 K. Thus, Fig. 10 have given the modified $\ln(I_s/T^2) - q^2\sigma^2/2k^2T^2$ versus q/kT plots for both values of σ_s. The best linear fitting to these modified experimental data is depicted by solid lines in Fig. 10 which represent the true activation energy plots in respective temperature ranges. The statistical analysis yielded effective mean BH $\bar{\Phi}_{Bo}$ of 0.61 eV (in the range 80–200 K) and 0.91 eV (in the range 220–340 K). These values match exactly with the mean BHs obtained from the Φ_{ap} versus $q/2kT$ plot in Fig. 9a. The interceptions at the ordinate give the Richardson constant A^* as 70.54 A/cm^2 K^2 (in 80–200 K range) and 7.49 A/cm^2 K^2 (in 220–340 K range) without using the temperature coefficient of the BHs. This value of the

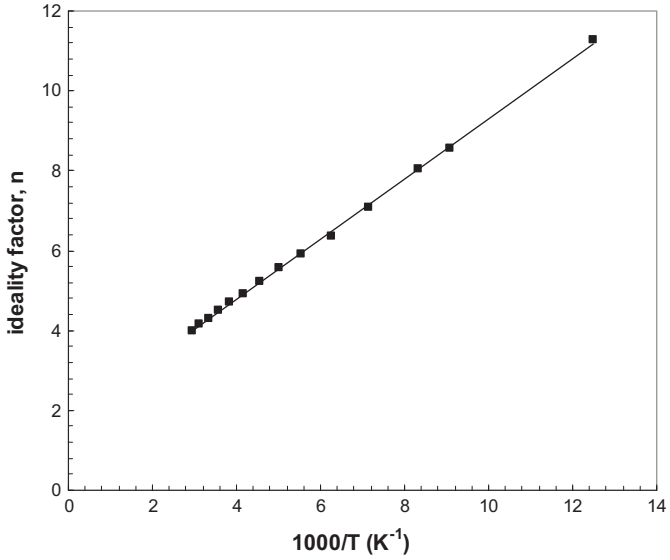

Fig. 11. The plot of n versus $1000/T$ of the Au/n-GaAs SBD for MBR.

Richardson constant 7.49 A/cm^2 K^2 is very close to the theoretical value of 8.16 A/cm^2 K^2 for Au/n-GaAs SBD.

3.2. Analysis of current–voltage (I–V) characteristics in the moderate bias region (MBR)

In the MBR, the changes in the Φ_{Bo} and n (Fig. 3b) is similar to LBR, but in MBR both the increase in Φ_{Bo} and $n\Phi_{Bo}$ with temperature cannot explain with TE and FE theories. Therefore, Φ_{Bo} versus q/kT plot was drawn to obtain an evidence of a GD of BHs. Thus, for the evaluation of the BH, one may also make use of the Richardson plot of saturation current. In Eq. (1), the I_s can be rearrange as Eq. (7). As can be seen in Table 1 and Fig. 11, n was change linearly with the inverse temperature and where (Eq. (3)) the n_0 and T_0 were found to be 1.77 and 752.4 K, respectively.

Fig. 12 shows a plot of nkT/q versus kT/q reporting the temperature dependence of the n, in which the straight line reported as

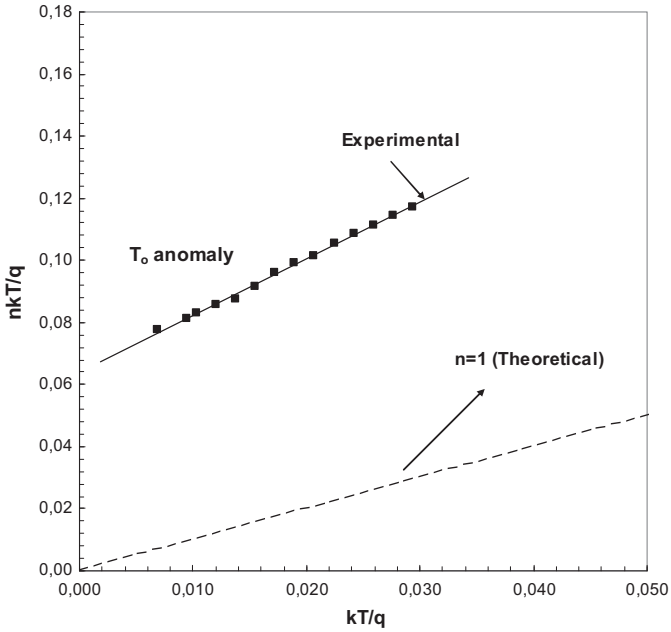

Fig. 12. Plots of the nkT/q versus kT/q of Au/n-GaAs SBD for LBR.

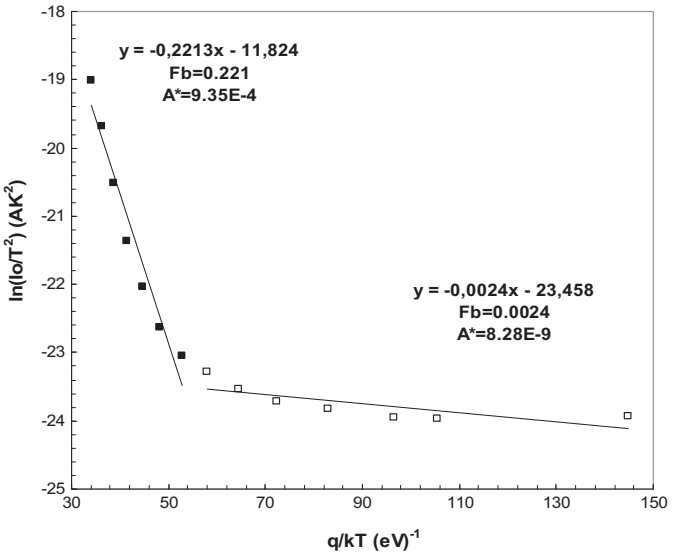

Fig. 13. Richardson plots of the $\ln(I_s/T^2)$ versus q/kT of Au/n-GaAs SBD for MBR.

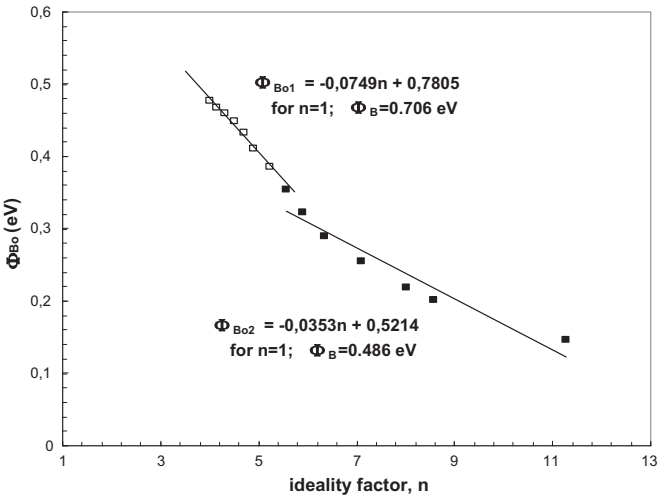

Fig. 14. Plot of the experimental BH versus n of Au/n-GaAs SBD for MBR.

a reference represents the ideal behavior of Schottky contact (i.e., with $n = 1$). It is clear that there is correlation between the experimental and the theoretical plots (nkT/q vs kT/q) for the Au/n-GaAs SBD for LBR. As can be seen from Fig. 12 the straight line fitted to the experimental values is not parallel to that of the ideal Schottky contact behavior. Such behavior can be explained T_o anomaly/effect and SBH inhomogeneity at M/S interface.

3.2.1. Inhomogeneous barrier analysis in the moderate bias regions

As shown in Fig. 13, in the MBR $\ln(I_s/T^2)$ versus q/kT plot, the conventional activation energy/Richardson plot show also two distinct linear region with different slopes similar to LBR.

In the first region (220–340 K), the values of the E_a and A^* were obtained from the slope and intercept of this straight-line as 0.221 eV and 9.35×10^{-4} A/cm^2 K^2, respectively, while in the second region (80–200 K), the values of E_d and A^* were obtained as 0.0024 eV and 8.28×10^{-9} A/cm^2 K^2, respectively. It is well known, for an electron, this value of A^* in Au/n-GaAs SBD is much lower than the theoretically value of 8.16 A/cm^2 K^2 for n-GaAs. Fig. 13 consists two BHs which are corresponding to the low and high barrier areas. Similar to LBR, at low temperatures, the carrier transport across MS contact would be preferentially through the lower barriers or patches in the potential distribution [11,37–39]. Fig. 14 shows a plot of the experimental BH versus n and it shows also two linear regions with different slopes which can be explained by the lateral inhomogeneities of the BHs [11,40]. In the first region (220–340 K), the extrapolation of the experimental Φ_{Bo} and n plot for $n = 1$ has given the value of 0.706 eV. In the second region (80–200 K), the extrapolation of the Φ_{Bo} and n plot for $n = 1$ has given the value of 0.486 eV. Thus, it can be said that the decrease of the Φ_{Bo} and increase of the n especially at low temperatures are possibly caused by the BH inhomogeneities. Therefore, such behaviors of Φ_{Bo} and n with temperature can be explained as above (for LBR).

In order to analysis of forward bias I–V characteristics based on barrier inhomogeneity, Werner and Güttler [20], show that introducing a GD in the BH with a mean value $\bar{\Phi}_{Bo}$ and standard deviation σ_s. Thus, the experimental Φ_{ap} versus $q/2kT$ and n_{ap} versus $q/2kT$ plots (Fig. 15) drawn by means of the data obtained from Fig. 2 respond to two lines instead of a single straight line with transition occurring at 200 K. As can be seen in Fig. 15, the intercept and slope of these straight lines given two sets of values of $\bar{\Phi}_{Bo}$ and σ_s as 0.65 eV and 0.1 V in the temperature range of 220–340 K (the

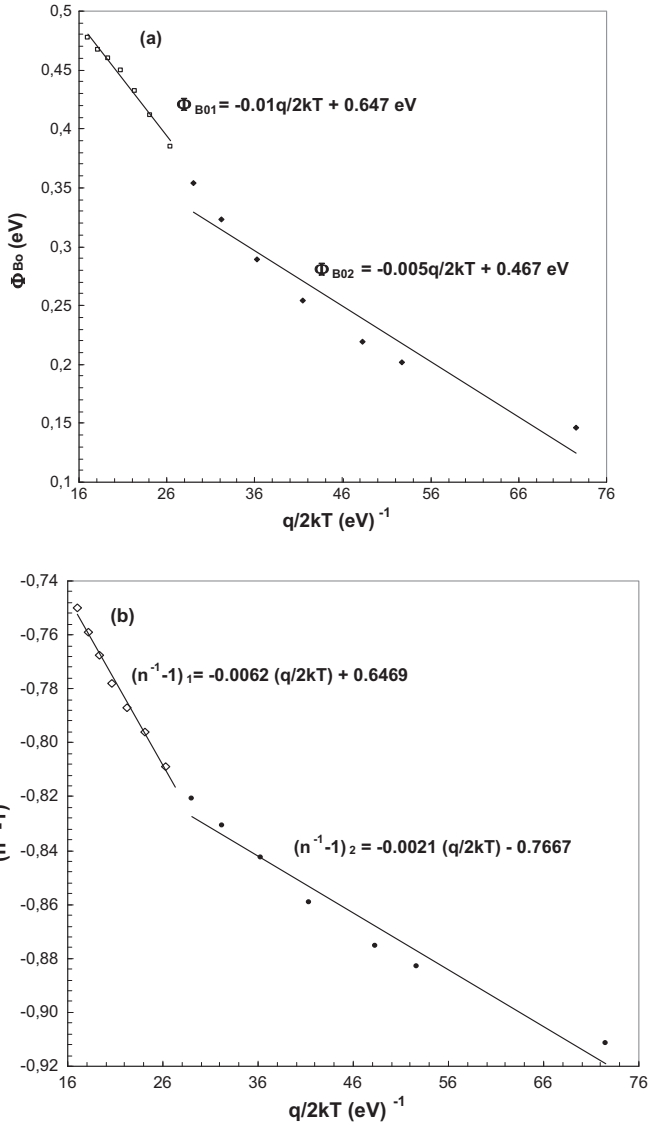

Fig. 15. (a) The apparent BH (Φ_{Bo} ($I-V$)) versus $q/2kT$ plot and (b) the ideality factor ($n^{-1}-1$) versus $q/2kT$ plot of Au/n-GaAs SBD for MBR.

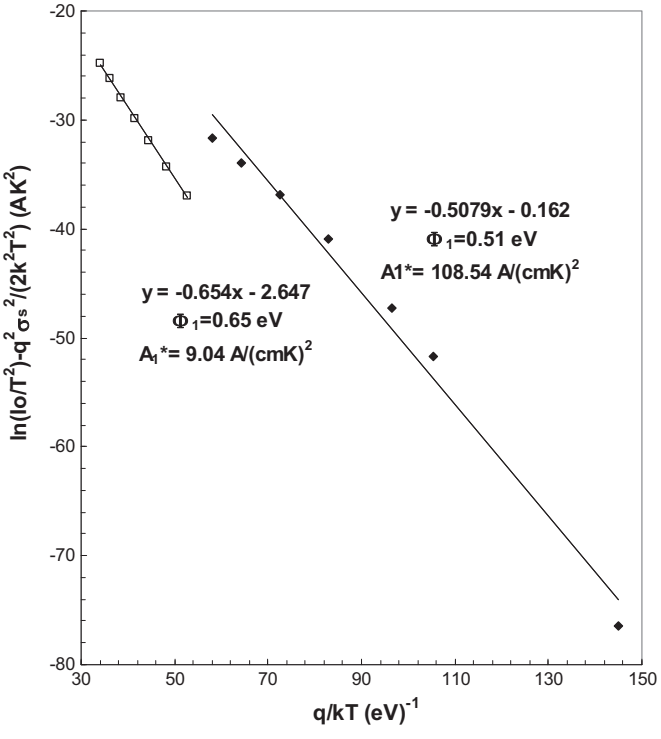

Fig. 16. Modified Richardson $\ln(I_0/T^2) - q^2\sigma_0{}^2/2k^2T^2$ versus q/kT plot of Au/n-GaAs SBD for MBR according to GD of BHs.

distribution 1), and as 0.47 eV and 0.07 V in the temperature range of 80–200 K (the distribution 2).

Similarly, as can be clearly seen from Fig. 15b, the $(n_{ap}{}^{-1} - 1)$ versus $q/2kT$ plot should also possess different characteristics in the two temperature ranges because the diode contains two BH distributions. The values of ρ_2 obtained from the intercepts of the experimental $(n_{ap}{}^{-1} - 1)$ versus $q/2kT$ plot are −0.65 V in 220–340 K range (the distribution 1) and −0.77 V in 80–200 K range (the distribution 2), whereas the values of ρ_3 from the slopes are 0.0062 V in 220–340 K range and 0.0021 V in 80–200 K range. The linear behavior of this plot demonstrates that the n indeed expresses the voltage deformation of the GD of the SBH. As can be seen from the $(n_{ap}{}^{-1} - 1)$ versus $q/2kT$, ρ_3 value or the slope of the distribution 1 is larger than the distribution 2. These results also show that, we may point out that the distribution 1 is wider and relatively higher BH with bias coefficients ρ_2 and ρ_3 being smaller and larger, respectively. Thus, we can say that the distribution 2 at very low temperatures may possibly arise due to some phase change taking place on cooling below a certain temperature. Similar to LBR, the obtained results in the MBR show that the BH is depend on temperature and two different current transport mechanisms or two different mean BHs may dominate in measured temperature range. Thus, the modified Richardson plots, $\ln(I_o/T^2) - q^2\sigma^2/2k^2T^2$ versus q/kT were obtained for both two values of σ_s obtained for the temperature ranges of 80–200 K and 220–340 K. The statistical analysis of Fig. 16 yielded effective mean BH $\bar{\Phi}_{Bo}$ of 0.65 eV (in the range 80–200 K) and 0.51 eV (in the range 220–340 K). These values match with the mean BHs obtained from the Φ_{ap} versus $q/2kT$ plot in Fig. 15a. The interceptions at the ordinate give the Richardson constant A^* as 108.54 A/cm^2 K^2 (in 80–200 K range) and 9.04 A/cm^2 K^2 (in 220–340 K range) without using the temperature coefficient of the BHs. This value of the Richardson constant 9.04 A/cm^2 K^2 is very close to the theoretical value of 8.16 A/cm^2 K^2 for Au/n-GaAs SBD.

As a result, for two applied bias regions the predominant current transport cannot explain only the TE and FE in our samples especially due to the high values of n. We think that the current transport mechanism in our sample (Au/n-GaAs SBD), can be well explained in the terms of two Gaussian distributions (GD1) and (GD2) BHs rather than the other mechanisms in the constant area which corresponding the high and low temperatures, respectively. On the other hand, all of these results implies that the investigation of the electrically influence of the I–V characteristics of the Schottky diodes is very important especially at low and moderate temperatures and applied bias voltages. In the current-transport mechanism for high temperatures, TE theory becomes more dominant due to gained thermal energy by charges and lowered in BH. Thus, I–V measurements especially at low temperatures are capable of revealing the nature of barrier inhomogeneities present in the contact area.

4. Conclusion

In order to obtain the detailed information on the current transport mechanisms of the Au/n-GaAs Schottky barrier diode (SBD), the current–voltage (I–V) characteristics were carried out in the temperature range of 80–340 K by the steps of 20 K. The ideality factor decreases from 5.43 to 1.29, while the barrier height increases from 0.18 eV to 0.64 eV with increasing temperature at 80–340 K. The ln(I) versus V curve at small forward current are almost parallel in this temperature range, which can be well explained by thermionic field emission (TFE) or field emission (FE) theories with the characteristic tunneling (FE or TFE) energy E_{oo} of 36 meV. Therefore, it can be said that the experimental I–V data quite well obey the field emission model rather than the thermionic emission or thermionic field emission model. On the other hand, the high values of n especially at low temperatures cannot be explained only TFE or FE theories. The linear relationship of BH versus n and the of $\ln(I_o/T^2) - q^2\sigma_o{}^2/2k^2T^2$ versus q/kT plots with two linear ranges shows that the temperature dependence of forward bias I–V characteristics of the Au/n-GaAs SBD can be successfully explained in terms of the TE mechanism with a double GD of BHs rather than the other mechanisms.

References

[1] Ö. Güllü, M. Biber, S. Duman, A. Türüt, Electrical characteristics of the hydrogen pre-annealed Au/n-GaAs Schottky barrier diodes as a function of temperature, Applied Surface Science 253 (2007) 7246–7253.
[2] F.A. Padovani, G.G. Sumner, Experimental study of gold–gallium arsenide Schottky barriers, Journal of Applied Physics 36 (1965) 3744–3747.
[3] F.A. Padovani, Graphical determination of the barrier height and excess temperature of a Schottky barrier, Journal of Applied Physics 37 (1966) 921–922.
[4] M.K. Hudait, P. Venkateswarlu, S.B. Krupanidhi, Electrical transport characteristics of Au/n-GaAs Schottky diodes on n-Ge at low temperatures, Solid-State Electronics 45 (2001) 133–141.
[5] A. Bengi, S. Altındal, S. Özçelik, T.S. Mammadov, Gaussian distribution of inhomogeneous barrier height in $Al_{0.24}Ga_{0.76}As$/GaAs structures, Physica B 396 (2007) 22–28.
[6] J.M. Borrego, R.J. Gutmann, S. Ashok, Interface state density in Au–nGaAs Schottky diodes, Solid-State Electronics 20 (1977) 125–132.
[7] R. Hackam, P. Harrop, Electrical properties of nickel-low-doped n-type gallium arsenide Schottky-barrier diodes, IEEE Transactions on IEEE Xplore – Electron Devices 19 (1972) 1231–1238.
[8] Zs.J. Horvath, Domination of the thermionic-field emission in the reverse I–V characteristics of n-type GaAs Schottky contacts, Journal of Applied Physics 64 (1988) 6780–6784.
[9] A.F. Ozdemir, A. Turut, A. Kokce, The double Gaussian distribution of barrier heights in Au/n-GaAs Schottky diodes from I–V–T characteristics, Semiconductor Science and Technology 21 (2006) 298–302.
[10] M. Soylu, F. Yakuphanoglu, Analysis of barrier height inhomogeneity in Au/n-GaAs Schottky barrier diodes by Tung Model, Journal of Alloys and Compounds 506 (2010) 418–422.
[11] H. Altuntaş, Ş. Altındal, H. Shtrikman, S. Özçelik, A detailed study of current–voltage characteristics in Au/SiO_2/n-GaAs in wide temperature range, Microelectronics Reliability 49 (2009) 904–911.
[12] Ş. Karataş, Ş. Altındal, Analysis of I–V characteristics on Au/n-type GaAs Schottky structures in wide temperature range, Materials Science and Engineering: B 122 (2005) 133–139.

[13] M.K. Hudait, S.B. Krupanidhi, Doping dependence of the barrier height and ideality factor of Au/n-GaAs Schottky diodes at low temperatures, Physica B 307 (2001) 125–137.
[14] W.P. Leroy, K. Opsomer, S. Forment, R.L. Van Meirhaneghe, The barrier height inhomogeneity in identically prepared Au/n-GaAs Schottky barrier diodes, Solid State Electronics 49 (2005) 878–883.
[15] A.T. Sharma, Shahnawaz, S. Kumar, Y.S. Katharria, D. Kanjilal, Barrier modification of Au/n-GaAs Schottky diode by swift heavy ion irradiation, Nuclear Instruments and Methods in Physics Research Section B 263 (2007) 424.
[16] A. Turut, Determination of barrier height temperature coefficient by Norde's method in ideal Co/n-GaAs Schottky contacts, Turkish Journal of Physics 36 (2012) 235–244.
[17] Ö. Güllü, M. Biber, R.L. Van Meirhaeghe, A. Türüt, Effects of the barrier metal thickness and pre-annealing on the characteristic parameters of Au/n-GaAs metal–semiconductor Schottky contacts, Thin Solid Films 616 (2008) 7851–7856.
[18] H. Korkut, N. Yıldırım, A. Türüt, Thermal annealing effects on *I–V–T* characteristics of sputtered Cr/n-GaAs diodes, Physica B 404 (2009) 4039–4044.
[19] R. Tung, Electron transport of inhomogeneous Schottky barriers, Applied Physics Letters 58 (1991) 2821–2823.
[20] J. Werner, H. Guttler, Barrier inhomogeneities at Schottky contacts, Journal of Applied Physics 69 (3) (1991) 1534.
[21] S. Shankar Naik, V. Rajagopal Reddy, Analysis of current–voltage–temperature (*I–V–T*) and capacitance–voltage–temperature (*C–V–T*) characteristics of Ni/Au Schottky contacts on n-type InP, Superlattices and Microstructures 48 (2010) 330–342.
[22] C. Kenney, K.C. Saraswat, B. Taylor, P. Majhi, Thermionic field emission explanation for nonlinear Richardson plots, IEEE Transactions on IEEE Xplore – Electron Devices 58 (2011) 2423–2429.
[23] Z. Harrabi, S. Jomni, L. Beji, A. Bouazizi, Distribution of barrier heights in Au/porous GaAs Schottky diodes from current–voltage–temperature measurements, Physica B 405 (2010) 3745–3750.
[24] M. Siva Pratap Reddy, A. Ashok Kumar, V. Rajagopal Reddy, Electrical transport characteristics of Ni/Pd/n-GaN Schottky barrier diodes as a function of temperature, Thin Solid Films 519 (2011) 3844–3850.
[25] E.H. Rhoderick, R.H. Williams, Metal-Semiconductor Contacts, Clarendon, Oxford, 1988.
[26] S.M. Sze, Physics of Semiconductor Devices, second ed., Wiley, New York, 1981.
[27] E. Arslan, Ş. Altındal, S. Özcelik, E. Ozbay, Dislocation-governed current-transport mechanism in (Ni/Au)–AlGaN/AlN/GaN heterostructures, Journal of Applied Physics 105 (2009) 023705–023712.
[28] A.N. Saxena, Forward current–voltage characteristics of Schottky barriers on n-type silicon, Surface Science 13 (1969) 151–171.
[29] S. Kar, S. Ashok, S.J. Fonash, Evidence of tunnel-assisted transport in non-degenerate MOS and semiconductor-oxide-semiconductor diodes at room temperature, Journal of Applied Physics 51 (1980) 3417–3422.
[30] M.O. Aboelfotoh, Temperature dependence of the Schottky-barrier height of tungsten on n-type and p-type silicon, Solid State Electronics 34 (1991) 51–55.
[31] A. Kassis, M. Saad, Analysis of multi-crystalline silicon solar cells at low illumination levels using a modified two-diode model, Solar Energy Materials and Solar Cells 94 (2010) 2108–2112.
[32] M. Saad, A. Kassis, Analysis of illumination-intensity-dependent *j–V* characteristics of ZnO/CdS/$CuGaSe_2$ single crystal solar cells, Solar Energy Materials and Solar Cells 77 (2003) 415–422.
[33] S. Demirezen, Ş. Altındal, İ. Uslu, Two diodes model and illumination effect on the forward and reverse bias *I–V* and *C–V* characteristics of Au/PVA (Bi-doped)/n-Si photodiode at room temperature, Current Applied Physics 13 (2013) 53–59.
[34] K. Ishaque, Z. Salam, H. Taheri, A. Shamsudin, A critical evaluation of EA computational methods for photovoltaic cell parameter extraction based on two diode model, Solar Energy 85 (2011) 1768–1779.
[35] G. Parish, R.A. Kennedy, G.A. Umana-Membreno, B.D. Nener, Localised defect-induced Schottky barrier lowering in n-GaN Schottky diodes, Solid State Electronics 52 (2008) 171–174.
[36] A.R. Arehart, A.A. Allerman, S.A. Ringle, Electrical characterization of n-type $Al_{0.30}Ga_{0.70}N$ Schottky diodes, Journal of Applied Physics 109 (2011) 114506–114516.
[37] O. Pakma, N. Serin, T. Serin, Ş. Altındal, The double Gaussian distribution of barrier heights in Al/TiO_2/p-Si (metal–insulator–semiconductor) structures at low temperatures, Journal of Applied Physics 104 (2008) 014501–014507.
[38] S. Demirezen, Z. Sönmez, U. Aydemir, Ş. Altındal, Effect of series resistance and interface states on the *I–V*, *C–V* and G/w-V characteristics in Au/Bi-doped polyvinyl alcohol (PVA)/n-Si Schottky barrier diodes at room temperature, Current Applied Physics 12 (2012) 266–272.
[39] Zs.J. Horvarth, Comment on Analysis of *I–V* measurements on $CrSi_2$-Si Schottky structures in a wide temperature range, Solid-State Electronics 39 (1996) 176–178.
[40] R.F. Schmitsdorf, T.U. Kampen, W. Mönch, Correlation between barrier height and interface structure of Schottky diodes, Surface Science 324 (1995) 249–256.
[41] T.U. Kampen, S. Park, D.R.T. Zahn, Barrier height engineering of Ag/GaAs(100) Schottky contacts by a thin organic interlayer, Applied Surface Science 190 (2002) 461–466.
[42] A.R.V. Roberts, D.A. Evans, Modification of GaAs Schottky diodes by thin organic interlayers, Applied Physics Letters 86 (2005) 072105–072108.
[43] S. Chand, J. Kumar, Evidence for the double distribution of barrier heights in Pd_2Si/n-Si Schottky diodes from *I–V–T* measurements, Semiconductor Science and Technology 11 (1996) 1203–1208.

Biographies

E. Özavcı received his BS and MS degree in electrical and electronics from Middle East Technical University (METU), Turkey, in 1983 and 1986. He is presently a Ph.D. student in physics at the Gazi University, Turkey. In 1984, he joined the Ankara Nuclear Research and Training Center at Turkish Atomic Energy Authority, Ankara, Turkey. Since 2003, he has been working at OGEM Ltd. Sti., Ankara, Turkey. He is interested in research and development projects.

S. Demirezen received his B.Ed. degree from Ondokuz Mayıs University, M.Sc. and Ph.D. degrees from Gazi University, Ankara, Turkey, in 1999, 2001, and 2010, respectively. His present research interest includes polymeric Schottky type electronic devices, metal–insulator–semiconductor junctions, solar cells, photodiode and their electrical and dielectric properties depend on frequency, temperature, radiation and illumination.

U. Aydemir received his B.Sc. degree from Gazi University's Physics program in 2007. He received his M.Sc. degree from same university's Semiconductor Technologies and Advanced Materials Program in 2009. Since January 2010 he is working as a researcher at Photonic Research and Application Center, Ankara, Turkey. His research interests are focused on semiconductor based devices such as organic solar cells, graphene–polymer nanocomposites, organic–inorganic Schottky diodes, etc.

Ş. Altındal received the B.Sc., M.Sc., and Ph.D. degrees from Gazi University, Ankara, Turkey, in 1982, 1989, and 1992, respectively, all in physics. His work for the Ph.D. degree was on solar cells. He is currently working as a professor with the Department of Physics, Faculty of Science, Gazi University. His current studies focused on polymeric Schottky type electronic devices and their electrical and dielectric properties depend on frequency, temperature, radiation and illumination.